



Published in final edited form as:

*Hum Brain Mapp.* 2015 October ; 36(10): 3793–3804. doi:10.1002/hbm.22878.

## Perfusion Shift from White to Gray Matter May Account for Processing Speed Deficits in Schizophrenia

Susan N. Wright<sup>1</sup>, L. Elliot Hong<sup>1</sup>, Anderson M. Winkler<sup>2</sup>, Joshua Chiappelli<sup>1</sup>, Katie Nugent<sup>1</sup>, Florian Muellerklein<sup>1</sup>, Xioming Du<sup>1</sup>, Laura M. Rowland<sup>1,3,6</sup>, Danny J. J. Wang<sup>4</sup>, and Peter Kochunov<sup>1,5,\*</sup>

<sup>1</sup>Department of Psychiatry, Maryland Psychiatric Research Center, University of Maryland School of Medicine, Baltimore, Maryland <sup>2</sup>Oxford Centre for Functional Magnetic Resonance Imaging of the Brain, University of Oxford, Oxford, United Kingdom <sup>3</sup>Department of Radiology and Radiological Sciences, Johns Hopkins University School of Medicine, Baltimore, Maryland <sup>4</sup>Department of Neurology, University of California, Los Angeles, California <sup>5</sup>Department of Physics, University of Maryland, Baltimore County, Maryland <sup>6</sup>Department of Psychology, University of Maryland, Baltimore County, Maryland

### Abstract

Reduced speed of cerebral information processing is a cognitive deficit associated with schizophrenia. Normal information processing speed (PS) requires intact white matter (WM) physiology to support information transfer. In a cohort of 107 subjects (47/60 patients/controls), we demonstrate that PS deficits in schizophrenia patients are explained by reduced WM integrity, which is measured using diffusion tensor imaging, mediated by the mismatch in WM/gray matter blood perfusion, and measured using arterial spin labeling. Our findings are specific to PS, and testing this hypothesis for patient-control differences in working memory produces no explanation. We demonstrate that PS deficits in schizophrenia can be explained by neurophysiological alterations in cerebral WM. Whether the disproportionately low WM integrity in schizophrenia is due to illness or secondary due to this disorder deserves further examination.

### Keywords

nicotine; DTI-FA; white matter; acute change; cognition; processing speed; attention

## INTRODUCTION

Reduced speed of information processing in schizophrenia patients is the core pathology of schizophrenia-association functional disabilities [Coyle et al., 2011; Dickinson et al., 2008; Hoyer et al., 2004; Knowles et al., 2010; Salthouse, 2000; Salthouse and Czaja, 2000]. The speed of cerebral information transfer depends on the integrity of myelinated cerebral white

\*Correspondence to: Peter Kochunov, Department of Psychiatry, Maryland Psychiatric Research Center, University of Maryland School of Medicine, Baltimore, MD. pkochunov@mprc.umaryland.edu.

Additional Supporting Information may be found in the online version of this article.

matter (WM). Patients with schizophrenia show significant deficits in WM integrity, as indexed by fractional anisotropy (FA) of water diffusion, and measured using diffusion tensor imaging (DTI). Reduced speed of information processing and reduced cerebral FA values are highly replicable findings in this disorder that are likely interlinked [Alba-Ferrara and de Erausquin, 2013; Ellison-Wright and Bullmore, 2009; Friedman et al., 2008; Glahn et al., 2013; Kubicki et al., 2007; Nazeri et al., 2013; Penke et al., 2010; Perez-Iglesias et al., 2011; Phillips et al., 2012]. In this study, we examined the link between processing speed (PS) and WM integrity in the context of the energy consumption. Specifically, we hypothesized that reduced WM integrity in patients may lead to alterations in the energy utilization between WM and gray matter (GM) compartments and this, in turn, may modulate functional deficits. The specificity of this effect was tested using two additional neuropsychological tests: working memory and Wechsler adult intelligence scale.

Information processing is an energy intensive process where the energy supply acts as an overall constraint [Harris and Attwell, 2012; Laughlin and Sejnowski, 2003]. Energy expended to support neurons in the cerebral GM is analogous to the energy that powers computers in a network, whereas the energy consumed by WM is analogous to the energy expended for signal transmission and network infrastructure. Using this analogy, support of the normal WM connectivity takes as much energy as the support of the “computational nodes” [Harris and Attwell, 2012; Lee et al., 2012; Vaishnavi et al., 2010]. Evolution drove the structure and physiology of cerebral WM to maximize efficiency of information processing [Hildebrand et al., 1993; Laughlin and Sejnowski, 2003; Wen and Chklovskii, 2005]. This is achieved through myelination, which increases the velocity of saltatory signal propagation (10–50 fold) [Hildebrand et al., 1993; Susuki, 2013] and reduces the metabolic burden on neuronal cells (5–10 fold) [Hildebrand et al., 1993; Miller et al., 2013; Susuki, 2013].

A reduced speed of information processing in schizophrenia patients is likely to be caused by impaired myelination [Davis et al., 2003; Mitkus et al., 2008; Susuki, 2013]. Deprived of the metabolic benefits of normal myelination, patients may exhibit a shift in the basal rate of metabolism from WM to GM. This can be tested by measuring the rate of resting metabolism or blood perfusion rate between WM and GM ( $R_{wm/gm}$ ). Simultaneous PET-MRI imaging demonstrates a high ( $r^2 > 0.7$ ) voxel-wise correlation between resting cerebral blood flow (CBF), measured by arterial spin labeling (ASL), and resting metabolism rate [Anazodo et al., 2015]. This replicates previous findings of the coupling between resting CBF and cerebral metabolism, albeit with some important regional variations [Bentourkia et al., 2000; Cha et al., 2013; Vaishnavi et al., 2010]. Therefore, we hypothesized that decline in WM integrity in patients may lead to the shift in basal WM and GM metabolism rates, and is reflected as a PS deficit.

To test this hypothesis, we used a digit-symbol coding task to measure cerebral signal conduction velocity [Ashe and Georgopoulos, 1994; Lancaster et al., 2005; Lutz et al., 2005]. The digit-symbol task was chosen because it shows the strongest effect size with schizophrenia of all the common cognitive tasks [Knowles et al., 2010]. We evaluated whether this effect was specific to processing by repeating analyses for working memory and Wechsler adult intelligence scale. We indexed WM integrity using DTI-FA, which is a

sensitive marker of WM integrity in schizophrenia [Ellison-Wright and Bullmore, 2009], including first-episode patients [Yao et al., 2013]. We collected resting CBF as the proxy measurement for energy consumption, and calculated  $R_{wm/gm}$  as the ratio of WM to GM CBF. This allowed us to study the shift in metabolic burden as the consequence of reduced WM integrity.

## METHODS

### Subjects

A total of 107 (65 M, 42 F) individuals participated in this study. Sixty one were healthy controls (35 males, 26 females,  $38.8 \pm 14.3$  years old) and 46 (30 males, 16 females,  $37.5 \pm 13.4$  years old) were patients diagnosed with schizophrenia. Additional clinical and demographic information is included in Table I. The patient and control groups did not differ in age, sex, BMI, or smoking frequency (Table I). Patients were recruited through the Maryland Psychiatric Research Center outpatient clinics. Healthy subjects were recruited through media advertisements. All subjects were evaluated with the Structured Clinical Interview for DSM-IV [First et al., 1996]. Patients were defined as individuals with the current Axis I schizophrenia diagnosis, while controls did not have any Axis I diagnosis. All but six patients were on antipsychotic medications. Participants completed clinical and neurocognitive testing as a part of the research study that included MRI. PS was assessed with the Digit Symbol Coding subtest of the WAIS-3 [Wechsler, 1997]. Additionally, we collected working memory assessment scores for all subjects using the Digit Sequencing task from the Brief Assessment of Cognition in Schizophrenia [Keefe et al., 2004]. Full WAIS-3 IQ scores were available for 77 subjects, including 24 patients (14 M, 10 F,  $33.5 \pm 13.7$ , years old) and 53 controls (24 M, 29 F,  $34.9 \pm 14.8$ ). Raw neuropsychological assessment scores were used, and corrections for age and gender were performed as part of the statistical modeling. Clinical symptoms in patients were measured by the 20-item Brief Psychiatric Rating Scale (BPRS), using a score of 1–7 for each item. Exclusion criteria for both groups included illicit substance and alcohol abuse and/or dependence, any major neurological diagnosis or events (head trauma, seizure, stroke, transient ischemic attack, hypertension, type-2 diabetes, and MRI contraindications). All experiments were performed with IRB approval, and all subjects signed an informed consent.

### Imaging and Data Analysis Protocols

All imaging was performed at the University of Maryland Center for Brain Imaging Research using a Siemens 3T TRIO MRI (Erlangen, Germany) and 32-channel phase array head coil.

**Diffusion tensor imaging**—High-angular resolution diffusion imaging DTI data was collected using a single-shot, echo-planar, single refocusing spin-echo, T2-weighted sequence with a spatial resolution of  $1.7 \times 1.7 \times 3.0$  mm. The sequence parameters were: TE/TR = 87/8,000 ms, FOV = 200 mm, axial slice orientation with 50 slices and no gaps, five  $b = 0$  images, and 64 isotropically distributed diffusion weighted directions with  $b = 700$  s/mm<sup>2</sup>. These parameters maximized the contrast-to-noise ratio for FA measurements [Phillips et al., 2012]. A tract-based spatial statistics (TBSS) method, distributed as a part of

the FMRIB Software Library (FSL) package, was used for tract-based analysis of diffusion anisotropy [Smith et al., 2006]. First, FA images were created by fitting the diffusion tensor to the motion and eddy current diffusion data. Average head motion during the DTI scans was measured during spatial alignments of diffusion-sensitized images to the  $b = 0$  image. The RMSDIFF program, distributed with FSL [Smith et al., 2004], was used to estimate the root mean square (RMS) movement distance between diffusion sensitized and  $b = 0$  images. All data passed quality assurance control of  $<3$  mm accumulated motion during the scan. There were no differences in the average motion per TR between patients and controls ( $0.42 \pm 0.21$  vs.  $0.43 \pm 0.20$ , for patients and controls, respectively). In the next step, all FA images were globally spatially normalized to the Johns Hopkins University (JHU) atlas that is distributed with the FSL package, version 5.0.1 [Wakana et al., 2004], and then nonlinearly aligned to a group-wise, minimal-deformation target (MDT) brain, as detailed elsewhere [Jahanshad et al., 2013]. The global spatial normalization was performed using a method distributed with the FSL package (FLIRT) [Smith et al., 2006], with 12 degrees of freedom. This step was performed to reduce the global intersubject variability in brain volumes prior to nonlinear alignment. The study sample group's MDT brain was identified by warping all individual brain images in the group to each other [Kochunov et al., 2001]. The MDT was selected as the image that minimizes the amount of the required deformation from other images in the group. Next, individual FA images were averaged to produce a group-average anisotropy image. This image was used to create a group-wise skeleton of WM tracts. The skeletonization procedure is a morphological operation that extracts the central axis of an object. This procedure was used to encode the central trajectory of the WM fiber-tracts with one-voxel thin sheaths.

FA images were thresholded at the level of  $FA = 0.20$  to eliminate likely non-WM voxels, and FA values were projected onto the group-wise skeleton of WM structures. This step accounts for residual misalignment among individual WM tracts. FA values were assigned to each point along the skeleton using the peak value found within a designated range perpendicular to the skeleton. The FA values vary rapidly perpendicular to the tract direction, but vary slowly along the tract direction. By assigning the peak value to the skeleton, this procedure effectively maps the center of individual WM tracts on the skeleton. This processing was performed under two constraints. First, a distance map was used to establish search borders for individual tracts. The borders were created by equally dividing the distance between two nearby tracts. Next, a multiplicative 20 mm full width at half-max Gaussian weighting was applied during the search to limit maximum projection distance from the skeleton [Smith et al., 2006].

**Pseudo-continuous arterial spin labeling imaging**—The detection of WM perfusion using ASL techniques was challenging in the past due to reduced volume coverage, low spatial resolution, and low signal-to-noise ratio of pulsed ASL sequences [van Gelderen et al., 2008]. However, recent technical developments in pulse sequence design and more sensitive phase-array coils have greatly improved the usefulness of this technique in clinical research [Wang and Licht, 2006; Wang et al., 2005]. We used a state-of-the-art Pseudo-continuous arterial spin labeling (pCASL) sequence that provided full brain coverage with high spatial resolution and excellent ASL signal-to-background noise ratio (SNR) ( $SNR >$

15). Specifically, we used a pCASL EPI with TE/TR = 16/4,000 ms, labeling duration = 2,100 ms, 24 contiguous slices with 5 mm thickness, matrix = 64 × 64, 3.4 × 3.4 × 5 mm resolution (FOV = 220 mm) labeling gradient of 0.6 G/cm, bandwidth = 1,594 Hz/pixel, labeling offset = 90 mm, post-labeling delay of 0.93 s [Wright et al., 2014]. A total of 68 alternating labeled and unlabeled image pairs were collected. The labeling duration and postlabeling delay sequence parameters were chosen empirically, as these maximized the overall labeling efficiency (contrast between labeled and unlabeled images) in five healthy volunteers 22–55 years of age. Equilibrium magnetization (M<sub>0</sub>) images were collected using a long TR = 10 s protocol [Wright et al., 2014]. T1-weighted images were collected using a protocol optimized to resolve the cortical ribbon using isotropic spatial sampling of 0.8 mm, voxel size = 0.5 mm<sup>3</sup>. T1-weighted contrast was achieved using a magnetization prepared sequence with an adiabatic inversion contrast-forming pulse (scan parameters: TE/TR/TI = 3.04/2,100/785 ms, flip angle = 11 degrees). ASL data were processed using the pipeline described elsewhere (<http://www.mccauslandcenter.sc.edu/CRNL/tools/asl>). In short, labeled and unlabeled ASL images were independently motion-corrected, and a combined mean image was computed and coregistered to the spatially normalized T1-weighted anatomical image. T1-weighted images were classified by tissue to produce the gray and WM tissue maps. Perfusion-weighted images were calculated by voxel-wise subtractions of unlabeled and labeled images, resulting in a mean perfusion-weighted image. Absolute WM perfusion or CBF<sub>WM</sub> (blood flow and perfusion are interchangeable terms here) quantification was calculated in native space from the mean perfusion images. Voxel-wise perfusion, in mL per 100 g per minute, was calculated under the assumption that the postlabel delay was longer than the arterial arrival time [Wang et al., 2002].

**Average and regional FA and CBF measurements**—Average FA measurements were calculated for each subject as the average value for the entire TBSS skeleton. The CBF maps were smoothed with a 6 mm FWHM Gaussian filter. The GM CBF map was made by masking the CBF image with the subject's GM tissue map (GM density > 50%), extracted from T1-weighted images, and then calculating the average for all non-zero voxels. The WM CBF map was calculated in two steps. First, the binary WM tissue map (WM density > 50%) was extracted. Then, it was eroded with a 10-mm spherical kernel to reduce contamination of WM CBF due to partial voxel averaging with GM and CSF [Mutsaerts et al., 2013]. Likewise, the average WM perfusion was calculated by averaging across the non-zero voxels. The whole brain  $R_{wm/gm}$  value was calculated as the ratio between WM and GM CBF values. Regional WM FA and CBF values were obtained using a population-based, 3D, DTI cerebral WM tract atlas developed at JHU, and distributed with the FSL package along the spatial course of 12 major WM tracts [Glahn et al., 2011; Kochunov et al., 2012; Wakana et al., 2004]. The per-tract  $R_{wm/gm}$  value was calculated by taking the ratio of per-track WM CBF to average GM CBF. We chose this approach because the JHU atlas indexes the core WM tracts that carry projections from many cortical areas at once.

## STATISTICAL ANALYSIS

Statistical analyses were performed in three steps: (1) testing overall group differences (2) association between PS and whole-brain average (3) regional neuroimaging measurements. In the first step, group differences in clinical, neuropsychological, and neuroimaging

measures were tested using a two-tailed *t*-test. In the second step, a mediation analysis was used to directly test the hypothesis that reduced WM integrity mediated PS via the mismatch in the WM and GM CBF. In the last step, we used general linear modeling to calculate the proportion of variance in the PS that could be attributed to the variability in WM integrity,  $R_{wm/gm}$ , and their interaction with the diagnosis. Finally, the specificity of our hypothesis was tested by repeating the analyses with the working memory and IQ scores.

### Mediation Effects on PS

Causal mediation analysis was used to directly test the hypothesis that reduced WM integrity mediated PS via the  $R_{wm/gm}$  [Imai et al., 2010; Tingley et al., 2013]. It tested the significance of the average causal mediation effect and the average direct effect of the “treatment” on the “outcome” via the “mediator.” In the first model, FA was chosen as the “treatment,” and  $R_{wm/gm}$  as the “mediator” (Fig. 1S, see Supporting Information). In the second model, the roles of FA and  $R_{wm/gm}$  were switched, while PS remained an outcome. This analysis was performed in the combined sample and in each of the groups separately; the age and gender were used as nuisance covariates. The causal mediation analysis was performed with the R package [R-Development-Core-Team, 2009], using the *mediation* library [Tingley et al., 2013]. The default suggested parameters, 1,000 permutations and a boot-strapping estimate of initial value, were used.

**Effects of FA and  $R_{wm/gm}$  on PS**—We studied the direct explanatory effects of FA and CBF on PS using general linear modeling, where PS was the dependent variable and FA,  $R_{w/gm}$ , diagnosis, and their interactions served as predictors. This analysis aimed to directly model the impact of the two neuroimaging measurements and the diagnosis status on PS. Specifically, we tested if the group difference in the PS remained significant after accounting for variance in the whole-brain averaged FA and CBF ratios [Eqs. (1) and (2)]. This modeling yielded the degree of variance explained, and tested the significance of the contribution from predictors to the variance in the PS. It also produced standardized coefficients (b) that estimated linear associations between PS variables and predictors.

$$PS \sim A + \beta_{FA} FA + \beta_{R_{\frac{W}{GM}}} R_{\frac{W}{GM}} + \beta_{dx} dx + \beta_{FA \times dx} FA \times dx + \beta_{R_{\frac{W}{GM}} \times dx} R_{\frac{W}{GM}} \cdot dx \quad (1)$$

$$R_{\frac{W}{GM}} = \frac{CBF_{WM}}{CBF_{GM}} \quad (2)$$

Next, the regional specificity of this association was probed using Eq. (3). This analysis was performed separately in each group for 10 regional WM measurements. In this ad hoc approach, regional  $R_{wm/gm}$  was obtained as the ratio of the pertract average WM CBF to the whole-brain GM CBF [Eq. (4)].

$$PS \sim A + \beta_{FA} tractFA^{tract} + \beta_{R_{\frac{W}{GM}}^{tract}} R_{\frac{W}{GM}}^{tract} \quad (3)$$

$$R_{\frac{WM}{GM}}^{tract} = \frac{CBF_{WM}^{tract}}{CBF_{GM}} \quad (4)$$

All modeling was performed with the R package [R-Development-Core-Team, 2009], using the Linear Effects Model library and the maximum likelihood estimation algorithm [Pinheiro et al., 2008; Tingley et al., 2013].

## RESULTS

Both groups were well-matched in age, sex, body weight, BMI, and smoking frequency (Table I). Patients had lower PS scores (two-tailed *t*-test,  $P = 10^{-7}$ ), whole-brain average FA ( $P = 0.02$ ), and  $R_{wm/gm}$  values ( $P = 0.002$ ) (Table I). In addition, patients had lower working memory and IQ scores ( $P = 0.02$  and  $0.003$ , respectively). Regionally, FA values in patients were only nominally reduced (Table 1S, see Supporting Information). There were no significant differences in global or regional GM or WM CBF values (Table I and Table 2S, see Supporting Information). The regional  $R_{wm/gm}$  values were suggestively significant for all of the tracts, and significantly different for three tracts: the genu, body, and splenium of corpus callosum, after correction for ten comparisons (Table 3S, see Supporting Information).

Both groups showed a similar pattern of association among neuroimaging and neurocognitive measurements. Whole-brain FA and  $R_{wm/gm}$  values were significantly and positively correlated in both groups ( $r = 0.52$ ,  $P = 3.5 \times 10^{-3}$  and  $r = 0.25$ ,  $P = 0.04$ , for patients and controls, respectively) (Fig. 1). Likewise, the PS scores were significantly correlated with the whole-brain  $R_{wm/gm}$  ( $r = 0.44$ ,  $P = 4.5 \times 10^{-3}$  and  $r = 0.41$ ,  $P = 1.1 \times 10^{-3}$ , in patients and controls, respectively) and FA values ( $r = 0.35$ ,  $P = 0.02$  and  $r = 0.36$ ,  $P = 0.005$ , in patients and controls, respectively) (Fig. 2).

The directionality of the association between PS and neuroimaging measurements was tested using a mediation model (Fig. 1S, Supporting Information).  $R_{wm/gm}$  was a significant mediator for the (FA  $\rightarrow$   $R_{W/GM}$   $\rightarrow$  PS) model in the combined ( $P = 0.01$ ) and patient samples ( $P = 0.04$ ), and approached significance in controls ( $P = 0.09$ ). The reverse mediation model ( $R_{W/GM}$   $\rightarrow$  FA  $\rightarrow$  PS) was not significant (Fig. 1S, Supporting Information). The age and sex were not significant covariates for the per group mediation model (all  $P > 0.2$ ).

The general linear modeling of PS as the function of FA,  $R_{w/gm}$ , diagnosis, and their interactions [Eq. (1); Table II] explained 38% of the variance in the combined model ( $F_{5,102} = 13.13$ ;  $P = 10^{-9}$ ).  $R_{w/gm}$  and FA were both significant predictors ( $P = 0.01$  and  $P = 0.004$ , respectively). The effects of diagnosis on PS were fully absorbed by the variance in neuroimaging measurements (Table II). Testing the model of regional FA and  $R_{W/GM}$  effects on PS [Eq. (3); Table III] also showed similarity among patients and controls, with genu, body of corpus callosum, and corona radiata (CR) showing significant differences in both groups (Table III).

Testing the specificity of our hypothesis was done by performing a correlation analysis between  $R_{w/gm}$ , working memory, and IQ scores. There was no significant association between  $R_{w/gm}$  and working memory scores in the whole sample or each group separately ( $r = 0.17, 0.10$  and  $0.25, P > 0.05$ , for the whole sample and controls and patients, respectively). Likewise, the interference analysis produced no significant association (Table II). In contrast, linear correlation between  $R_{w/gm}$  and IQ scores were significant ( $r = 0.42, 0.32$ , and  $0.54, P < 0.05$ , for the whole sample and controls and patients, respectively). However, the partial correlation coefficients, corrected by processing speed, were not significant ( $Pr = 0.25, 0.03$ , and  $0.32, P > 0.05$ ).

## DISCUSSION

In this study, we observed that the neuroimaging measurements of reduced WM integrity explained patient-control differences in the speed of information processing in schizophrenic patients. The WM integrity measurements captured the diagnosis-related variance, with similar trends observed in both groups. This suggests that reduced speed of information processing is a function of poor WM integrity in both groups, and was not specifically linked to schizophrenia. Directionality tests suggest that structural deficits, measured by reduced FA, led to the shift in CBF ratio ( $R_{WM/GM}$ ), which, in turn, mediated the processing speed. The analysis of regional trends further corroborated our hypothesis by demonstrating that reduced integrity of associative, rather than motor and sensory, WM regions may explain the processing speed deficits in both groups. This is consistent with previous research showing that the integrity of associative WM fibers that carry multimodal, higher order functional information, is critical for maintaining normal speed of information processing [Borghesani et al., 2013; Genova et al., 2013; Kochunov et al., 2010; Llufriu et al., 2012; Peters et al., 2014].  $R_{WM/GM}$  appeared to be specifically associated with processing speed. We tested the specificity of this association by repeating the analyses with two other neurocognitive measurements that are reduced in schizophrenia patients, working memory and IQ. We observed no significant association between  $R_{WM/GM}$  and working memory. Significant association between  $R_{WM/GM}$  and IQ scores were modulated by the impact of processing speed and IQ and lost significance once effects of processing speed were accounted for. Overall, our results constitute the testing of a neurobiological model of reduced processing speed, and suggest that the processing speed deficits in schizophrenic patients are governed by the same neurobiological mechanisms as controls.

The cerebral disconnectivity in schizophrenic patients [Friston and Frith, 1995; Lillrank et al., 1995; Repovs et al., 2011; Weinberger, 1996] is often characterized by deficits in WM integrity [Alba-Ferrara and de Erausquin, 2013; White et al., 2013]. A consequence of this disconnectivity is a profound deficit in the speed of information processing in schizophrenic patients [Knowles et al., 2010] that may also underlie impairments in other cognitive functions [Brebion et al., 1998; Coyle et al., 2011; Salthouse, 2000, 2009]. Processing speed depends on the integrity of cerebral WM, and is strongly associated with measurements of conduction velocity, such as cerebral and interhemispheric conduction velocities [Bartzokis et al., 2003, 2010; Horsfield and Jones, 2002; Lancaster et al., 2003, 2005; Llufriu et al., 2012; Nowicka and Tacikowski, 2009; Waxman and Bennett, 1972].

Processing speed declines during normal aging, and findings from aging research may help us interpret the neurobiological mechanism of this deficit in schizophrenia. The decline of the processing speed in aging is driven by the reduction in the propagation speed of action potentials across cortical networks [Ashe and Georgopoulos, 1994; Lutz et al., 2005]. In parallel, structural measurements of WM integrity, such as FA values, explain ~15% of the variance in the processing speed [Borghesani et al., 2013; Kochunov et al., 2009b; Peters et al., 2014; Schiavone et al., 2009]. The link between reduced processing speed deficits and WM integrity is further strengthened by observations in schizophrenic patients. A reduction in processing speed and WM FA values occur in parallel prior to onset of schizophrenia in adolescents at high clinical risk for psychosis [Bachman et al., 2012; Bloemen et al., 2010; Carletti et al., 2012; Karlsgodt et al., 2009]. Additionally, schizophrenic patients experience an accelerated (up to two times) rate of aging in cerebral WM compared to controls [Friedman et al., 2008; Mori et al., 2007; Phillips et al., 2012; Wright et al., 2014]. This accelerated decline in WM integrity may explain why adult schizophrenic patients exhibit a processing speed performance comparable to normal controls twice their age [Bonner-Jackson et al., 2011; Loewenstein et al., 2011].

Here, we proposed a novel measurement:  $R_{WM/GM}$  as the ratio of WM to GM perfusion to be a proxy index for the resting energy consumption. Perfusion refers to the microcirculation of blood to supply tissues with nutrients, and when measured during resting state, is coupled with glucose utilization and metabolism [Biagi et al., 2007; Cha et al., 2013; Musiek et al., 2011]. Our use of  $R_{WM/GM}$  was intended to replicate previous findings that showed significantly altered WM/GM glucose metabolism ratios in schizophrenic patients [Altamura et al., 2013]. Our findings are consistent with those reported by Altamura et al., who attributed the reduced WM/GM uptake ratio in schizophrenia to defects in energy usage and structural alterations in WM integrity [Altamura et al., 2013].

Regarding the regional pattern of associations, regional FA and  $R_{WM/GM}$  values from associative WM, including the corpus callosum, CR, and cingulate, explained the highest proportion of processing speed in both groups. Measurements for the WM tracts that carry motor and sensory fibers, such as the internal and external capsules (IC and EC), showed the weakest associations with processing speed in both groups. Overall, our findings are novel and may offer biological insight to the causes of deficits in processing speed in schizophrenia. It suggests that reduced structural WM integrity in patients may lead to a shift of energy consumption from WM to GM, and this in turn leads to reduced processing speed.

## LIMITATIONS AND FUTURE DIRECTIONS

This article presents novel and exciting findings that posit  $R_{WM/GM}$  as a prospective neuroimaging endopheno-type that may clarify the core cognitive deficit of schizophrenia. However, a replication in an independent cohort is necessary to ensure that the findings in this study were not caused by unforeseen factors. We attempted to minimize the impact of common age-related metabolic disorders such as hypertension, diabetes, heart disorders, and stroke by excluding affected subjects. We cannot rule out effects from chronic antipsychotic exposure in patients. The correlations between processing speed, whole-brain FA and

$R_{WM/GM}$ , and current antipsychotic medication dose, as calculated by chlorpromazine equivalent (CPZ), were not significant ( $r < 0.1$ ;  $P > 0.6$ ). Similar findings are observed for correlations between CPZ and regional FA and  $R_{WM/GM}$  measurements (all  $r \leq 0.2$ , all  $P > 0.3$ ). Additionally, there were no differences in the processing speed or imaging measurements between medicated and unmedicated patients (all  $P > 0.6$ ). Nonetheless, the present design would not allow for a differentiation or even speculation if the findings were due to the schizophrenia etiology, or by the chronic antipsychotic medication exposure. Ascertainment of a large antipsychotic-naïve patient group across different ages to rule out medication effects would be required to answer this question.

The use of an ASL technique to measure  $R_{WM/GM}$  to index the shift in metabolic burden carries its own limitations. ASL is a signal-to-background noise ratio (SNR)-limited technique leading to long acquisition times and coarse spatial resolution. Nonetheless, a study that used a similar ASL protocol for mapping CBF while simultaneously using MRI-PET imaging reported excellent overall correlation ( $r^2 > 0.7$ ) between ASL-measured perfusion and PET-measured cerebral glucose uptake [Anazodo et al., 2015]. Further improvements in ASL imaging and analysis approaches, such as background suppressed pCASL, can significantly improve SNR in cerebral WM and reduce acquisition times in half versus conventional pCASL techniques, thus, making  $R_{WM/GM}$  measurements practical in as little as 2–3 min [van Osch et al., 2009].

Another potential limitation is that the reduced thickness of cortical GM can produce an apparent reduction in cortical perfusion measurements, due to partial volume averaging artifact [Kochunov et al., 2009a]. In the post hoc analysis, we measured cortical GM thickness using Free-Surfer [Fischl and Dale, 2000], and observed no significant differences in the average GM thickness between groups ( $2.45 \pm 0.13$  and  $2.42 \pm 0.13$ ,  $P = 0.8$ , for patients and controls, respectively). Consistent with that, there were no significant group-wise differences ( $P = 0.5$ ) in the average GM CBF measurements (Table I). For future studies, the use of partial voxel averaging correction algorithms, such as one proposed for ASL by Asllani and colleagues, may help to overcome this limitation [Asllani et al., 2008].

## Supplementary Material

Refer to Web version on PubMed Central for supplementary material.

## Acknowledgments

Contract grant sponsor: National Institute of Health; Contract grant numbers: R01MH085646, R01DA027680 (to L.E.H) R01MH094520 (to L.M.R.), and R01EB015611 (to P.K.); Contract grant sponsor: NIH Institutes contributing to the Big Data to Knowledge (BD2K) Initiative, including the NIBIB and NCI (Consortium grant); Contract grant number: U54 EB020403; Contract grant sponsor: National Institute of Health; Contract grant numbers: P50MH103222 and T32MH067533

## References

Alba-Ferrara LM, de Erausquin GA. What does anisotropy measure? Insights from increased and decreased anisotropy in selective fiber tracts in schizophrenia. *Front Integr Neurosci*. 2013; 7:9. [PubMed: 23483798]

- Altamura AC, Bertoldo A, Marotta G, Paoli RA, Caletti E, Dragogna F, Buoli M, Baglivo V, Mauri MC, Brambilla P. White matter metabolism differentiates schizophrenia and bipolar disorder: A preliminary PET study. *Psychiatry Res.* 2013; 214:410–414. [PubMed: 24144506]
- Anazodo UC, Thiessen JD, Ssali T, Mandel J, Gunther M, Butler J, Pavlosky W, Prato FS, Thompson RT, St Lawrence KS. Feasibility of simultaneous whole-brain imaging on an integrated PET-MRI system using an enhanced 2-point Dixon attenuation correction method. *Front Neurosci.* 2015; 8:434. [PubMed: 25601825]
- Ashe J, Georgopoulos AP. Movement parameters and neural activity in motor cortex and area 5. *Cereb Cortex.* 1994; 4:590–600. [PubMed: 7703686]
- Asllani I, Borogovac A, Brown TR. Regression algorithm correcting for partial volume effects in arterial spin labeling MRI. *Magn Reson Med.* 2008; 60:1362–1371. [PubMed: 18828149]
- Bachman P, Niendam TA, Jalbrzikowski M, Park CY, Daley M, Cannon TD, Bearden CE. Processing speed and neurodevelopment in adolescent-onset psychosis: Cognitive slowing predicts social function. *J Abnorm Child Psychol.* 2012; 40:645–654. [PubMed: 22134489]
- Bartzokis G, Cummings JL, Sultzer D, Henderson VW, Nuechterlein KH, Mintz J. White matter structural integrity in healthy aging adults and patients with Alzheimer disease: A magnetic resonance imaging study. *Arch Neurol.* 2003; 60:393–398. [PubMed: 12633151]
- Bartzokis G, Lu PH, Tingus K, Mendez MF, Richard A, Peters DG, Oluwadara B, Barrall KA, Finn JP, Villablanca P, Thompson PM, Mintz J. Lifespan trajectory of myelin integrity and maximum motor speed. *Neurobiol Aging.* 2010; 31:1554–1562. [PubMed: 18926601]
- Bentourkia M, Bol A, Ivanoiu A, Labar D, Sibomana M, Coppens A, Michel C, Cosnard G, De Volder AG. Comparison of regional cerebral blood flow and glucose metabolism in the normal brain: Effect of aging. *J Neurol Sci.* 2000; 181:19–28. [PubMed: 11099707]
- Biagi L, Abbruzzese A, Bianchi MC, Alsop DC, Del Guerra A, Tosetti M. Age dependence of cerebral perfusion assessed by magnetic resonance continuous arterial spin labeling. *J Magn Reson Imaging.* 2007; 25:696–702. [PubMed: 17279531]
- Bloemen OJ, de Koning MB, Schmitz N, Nieman DH, Becker HE, de Haan L, Dingemans P, Linszen DH, van Amelsvoort TA. White-matter markers for psychosis in a prospective ultra-high-risk cohort. *Psychol Med.* 2010; 40:1297–1304. [PubMed: 19895720]
- Bonner-Jackson A, Grossman LS, Harrow M, Rosen C. Neurocognition in schizophrenia: A 20-year multi-follow-up of the course of processing speed and stored knowledge. *Compr Psychiatry.* 2011; 51:471–479. [PubMed: 20728003]
- Borghesani PR, Madhyastha TM, Aylward EH, Reiter MA, Swarny BR, Schaie KW, Willis SL. The association between higher order abilities, processing speed, and age are variably mediated by white matter integrity during typical aging. *Neuropsychologia.* 2013; 51:1435–1444. [PubMed: 23507612]
- Brebion G, Amador X, Smith MJ, Gorman JM. Memory impairment and schizophrenia: The role of processing speed. *Schizophr Res.* 1998; 30:31–39. [PubMed: 9542786]
- Carletti F, Woolley JB, Bhattacharyya S, Perez-Iglesias R, Fusar Poli P, Valmaggia L, Broome MR, Bramon E, Johns L, Giampietro V, Williams SC, Barker GJ, McGuire PK. Alterations in white matter evident before the onset of psychosis. *Schizophr Bull.* 2012; 38:1170–1179. [PubMed: 22472474]
- Cha YH, Jog MA, Kim YC, Chakrapani S, Kraman SM, Wang DJ. Regional correlation between resting state FDG PET and pCASL perfusion MRI. *J Cereb Blood Flow Metab.* 2013; 33:1909–1914. [PubMed: 23963370]
- Coyle TR, Pillow DR, Snyder AC, Kochunov P. Processing speed mediates the development of general intelligence (g) in adolescence. *Psychol Sci.* 2011; 22:1265–1269. [PubMed: 21931154]
- Davis KL, Stewart DG, Friedman JI, Buchsbaum M, Harvey PD, Hof PR, Buxbaum J, Haroutunian V. White matter changes in schizophrenia: Evidence for myelin-related dysfunction. *Arch Gen Psychiatry.* 2003; 60:443–456. [PubMed: 12742865]
- Dickinson D, Ragland JD, Gold JM, Gur RC. General and specific cognitive deficits in schizophrenia: Goliath defeats David? *Biol Psychiatry.* 2008; 64:823–827. [PubMed: 18472089]
- Ellison-Wright I, Bullmore E. Meta-analysis of diffusion tensor imaging studies in schizophrenia. *Schizophr Res.* 2009; 108:3–10. [PubMed: 19128945]

- First, MB.; Spitzer Robert, L.; Gibbon, Miriam; Williams Janet, BW. Structured Clinical Interview for DSM-IV Axis I Disorders, Clinical Version (SCID-CV). Washington, DC: American Psychiatric Press, Inc; 1996.
- Fischl B, Dale AM. Measuring the thickness of the human cerebral cortex from magnetic resonance images. *Proc Natl Acad Sci USA*. 2000; 97:11050–11055. [PubMed: 10984517]
- Friedman JI, Tang C, Carpenter D, Buchsbaum M, Schmeidler J, Flanagan L, Golembo S, Kanellopoulou I, Ng J, Hof PR, Harvey PD, Tsopelas ND, Stewart D, Davis KL. Diffusion tensor imaging findings in first-episode and chronic schizophrenia patients. *Am J Psychiatry*. 2008; 165:1024–1032. [PubMed: 18558643]
- Friston KJ, Frith CD. Schizophrenia: A disconnection syndrome? *Clin Neurosci*. 1995; 3:89–97. [PubMed: 7583624]
- Genova HM, DeLuca J, Chiaravalloti N, Wylie G. The relationship between executive functioning, processing speed, and white matter integrity in multiple sclerosis. *J Clin Exp Neuropsychol*. 2013; 35:631–641. [PubMed: 23777468]
- Glahn DC, Curran JE, Winkler AM, Carless MA, Kent JW Jr, Charlesworth JC, Johnson MP, Goring HH, Cole SA, Dyer TD, Moses EK, Olvera RL, Kochunov P, Duggirala R, Fox PT, Almasy L, Blangero J. High dimensional endophenotype ranking in the search for major depression risk genes. *Biol Psychiatry*. 2011; 71:6–14. [PubMed: 21982424]
- Glahn DC, Kent JW Jr, Sprooten E, Diego VP, Winkler AM, Curran JE, McKay DR, Knowles EE, Carless MA, Goring HH, Dyer TD, Olvera RL, Fox PT, Almasy L, Charlesworth J, Kochunov P, Duggirala R, Blangero J. Genetic basis of neurocognitive decline and reduced white-matter integrity in normal human brain aging. *Proc Natl Acad Sci USA*. 2013; 110:19006–19011. [PubMed: 24191011]
- Harris JJ, Attwell D. The energetics of CNS white matter. *J Neurosci*. 2012; 32:356–371. [PubMed: 22219296]
- Hildebrand C, Remahl S, Persson H, Bjartmar C. Myelinated nerve fibres in the CNS. *Prog Neurobiol*. 1993; 40:319–384. [PubMed: 8441812]
- Horsfield MA, Jones DK. Applications of diffusion-weighted and diffusion tensor MRI to white matter diseases—A review. *NMR Biomed*. 2002; 15:570–577. [PubMed: 12489103]
- Hoyer WJ, Stawski RS, Wasylshyn C, Verhaeghen P. Adult age and digit symbol substitution performance: A meta-analysis. *Psychol Aging*. 2004; 19:211–214. [PubMed: 15065945]
- Imai K, Keele L, Tingley D. A general approach to causal mediation analysis. *Psychol Methods*. 2010; 15:309–334. [PubMed: 20954780]
- Jahanshad N, Kochunov P, Sprooten E, Mandl RC, Nichols TE, Almasy L, Blangero J, Brouwer RM, Curran JE, de Zubicaray GI, Duggirala R, Fox PT, Hong LE, Landman BA, Martin NG, McMahon KL, Medland SE, Mitchell BD, Olvera RL, Peterson CP, Starr JM, Sussmann JE, Toga AW, Wardlaw JM, Wright MJ, Hulshoff Pol HE, Bastin ME, McIntosh AM, Deary IJ, Thompson PM, Glahn DC. Multi-site genetic analysis of diffusion images and voxelwise heritability analysis: A pilot project of the ENIGMA-DTI working group. *Neuroimage*. 2013; 81:455–469. [PubMed: 23629049]
- Karlsgodt KH, Niendam TA, Bearden CE, Cannon TD. White matter integrity and prediction of social and role functioning in subjects at ultra-high risk for psychosis. *Biol Psychiatry*. 2009; 66:562–569. [PubMed: 19423081]
- Keefe RS, Goldberg TE, Harvey PD, Gold JM, Poe MP, Coughenour L. The brief assessment of cognition in schizophrenia: Reliability, sensitivity, and comparison with a standard neurocognitive battery. *Schizophr Res*. 2004; 68:283–297. [PubMed: 15099610]
- Knowles EE, David AS, Reichenberg A. Processing speed deficits in schizophrenia: Reexamining the evidence. *Am J Psychiatry*. 2010; 167:828–835. [PubMed: 20439390]
- Kochunov P, Lancaster JL, Thompson P, Woods R, Mazziotta J, Hardies J, Fox P. Regional spatial normalization: Toward an optimal target. *J Comput Assist Tomogr*. 2001; 25:805–816. [PubMed: 11584245]
- Kochunov P, Ramage AE, Lancaster JL, Robin DA, Narayana S, Coyle T, Royall DR, Fox P. Loss of cerebral white matter structural integrity tracks the gray matter metabolic decline in normal aging. *Neuroimage*. 2009a; 45:17–28. [PubMed: 19095067]

- Kochunov P, Robin D, Royall D, Lancaster J, Kochunov V, Coyle T, Schlosser A, Fox P. Can structural MRI cerebral health markers track cognitive trends in executive control function during normal maturation and adulthood? *Hum Brain Mapp.* 2009b; 30:2581–2594. [PubMed: 19067326]
- Kochunov P, Coyle T, Lancaster J, Robin DA, Hardies J, Kochunov V, Bartzokis G, Stanley J, Royall D, Schlosser AE, Null M, Fox PT. Processing speed is correlated with cerebral health markers in the frontal lobes as quantified by neuroimaging. *Neuroimage.* 2010; 49:1190–1199. [PubMed: 19796691]
- Kochunov P, Williamson DE, Lancaster J, Fox P, Cornell J, Blangero J, Glahn DC. Fractional anisotropy of water diffusion in cerebral white matter across the lifespan. *Neurobiol Aging.* 2012; 33:9–20. [PubMed: 20122755]
- Kubicki M, McCarley R, Westin CF, Park HJ, Maier S, Kikinis R, Jolesz FA, Shenton ME. A review of diffusion tensor imaging studies in schizophrenia. *J Psychiatr Res.* 2007; 41:15–30. [PubMed: 16023676]
- Lancaster JL, Andrews T, Hardies LJ, Dodd S, Fox PT. Three-pool model of white matter. *J Magn Reson Imaging.* 2003; 17:1–10. [PubMed: 12500269]
- Lancaster JL, Cody JD, Andrews T, Hardies LJ, Hale DE, Fox PT. Myelination in children with partial deletions of chromosome 18q. *AJNR Am J Neuroradiol.* 2005; 26:4472454.
- Laughlin SB, Sejnowski TJ. Communication in neuronal networks. *Science.* 2003; 301:1870–1874. [PubMed: 14512617]
- Lee Y, Morrison BM, Li Y, Lengacher S, Farah MH, Hoffman PN, Liu Y, Tsingalia A, Jin L, Zhang PW, Pellerin L, Magistretti PJ, Rothstein JD. Oligodendroglia metabolically support axons and contribute to neurodegeneration. *Nature.* 2012; 487:443–448. [PubMed: 22801498]
- Lillrank SM, Lipska BK, Weinberger DR. Neurodevelopmental animal models of schizophrenia. *Clin Neurosci.* 1995; 3:98–104. [PubMed: 7583625]
- Llufriu S, Blanco Y, Martinez-Heras E, Casanova-Molla J, Gabilondo I, Sepulveda M, Falcon C, Berenguer J, Bargallo N, Villoslada P, Graus F, Valls-Sole J, Saiz A. Influence of corpus callosum damage on cognition and physical disability in multiple sclerosis: A multimodal study. *PLoS One.* 2012; 7:e37167. [PubMed: 22606347]
- Loewenstein DA, Czaja SJ, Bowie CR, Harvey PD. Age-associated differences in cognitive performance in older patients with schizophrenia: A comparison with healthy older adults. *Am J Geriatr Psychiatry.* 2011; 20:29–40. [PubMed: 22130385]
- Lutz K, Koeneke S, Wustenberg T, Jancke L. Asymmetry of cortical activation during maximum and convenient tapping speed. *Neurosci Lett.* 2005; 373:61–66. [PubMed: 15555778]
- Miller DJ, Duka T, Stimpson CD, Schapiro SJ, Baze WB, McArthur MJ, Fobbs AJ, Sousa AM, Sestan N, Wildman DE, Lipovich L, Kuzawa CW, Hof PR, Sherwood CC. Prolonged myelination in human neocortical evolution. *Proc Natl Acad Sci USA.* 2013; 109:16480–16485. [PubMed: 23012402]
- Mitkus SN, Hyde TM, Vakkalanka R, Kolachana B, Weinberger DR, Kleinman JE, Lipska BK. Expression of oligodendrocyte-associated genes in dorsolateral prefrontal cortex of patients with schizophrenia. *Schizophr Res.* 2008; 98:129–138. [PubMed: 17964117]
- Mori T, Ohnishi T, Hashimoto R, Nemoto K, Moriguchi Y, Noguchi H, Nakabayashi T, Hori H, Harada S, Saitoh O, Matsuda H, Kunugi H. Progressive changes of white matter integrity in schizophrenia revealed by diffusion tensor imaging. *Psychiatry Res.* 2007; 154:133–145. [PubMed: 17276660]
- Musiek ES, Chen Y, Korczykowski M, Saboury B, Martinez PM, Reddin JS, Alavi A, Kimberg DY, Wolk DA, Julin P, Newberg AB, Arnold SE, Detre JA. Direct comparison of fluorodeoxyglucose positron emission tomography and arterial spin labeling magnetic resonance imaging in Alzheimer's disease. *Alzheimers Dement.* 2011; 8:51–59. [PubMed: 22018493]
- Mutsaerts HJMM, Richard E, Heijtel DFR, van Osch MJP, Majoie CBLM, Nederveen AJ. Gray matter contamination in arterial spin labeling white matter perfusion measurements in patients with dementia. *NeuroImage Clin.* 2013; 4:139–144. [PubMed: 24371796]
- Nazeri A, Mallar Chakravarty M, Felsky D, Lobaugh NJ, Rajji TK, Mulsant BH, Voineskos AN. Alterations of superficial white matter in schizophrenia and relationship to cognitive performance. *Neuropsychopharmacology.* 2013; 38:1954–1962. [PubMed: 23591167]

- Nowicka A, Tacikowski P. Transcallosal transfer of information and functional asymmetry of the human brain. *Laterality*. 2009; 16:35–74. [PubMed: 19657954]
- Penke L, Munoz Maniega S, Murray C, Gow AJ, Hernandez MC, Clayden JD, Starr JM, Wardlaw JM, Bastin ME, Deary IJ. A general factor of brain white matter integrity predicts information processing speed in healthy older people. *J Neurosci*. 2010; 30:7569–7574. [PubMed: 20519531]
- Perez-Iglesias R, Tordesillas-Gutierrez D, McGuire PK, Barker GJ, Roiz-Santanez R, Mata I, de Lucas EM, Rodriguez-Sanchez JM, Ayasa-Arriola R, Vazquez-Barquero JL, Crespo-Facorro B. White matter integrity and cognitive impairment in first-episode psychosis. *Am J Psychiatry*. 2011; 167:451–458. [PubMed: 20160006]
- Peters BD, Ikuta T, Derosse P, John M, Burdick KE, Gruner P, Prendergast DM, Szeszko PR, Malhotra AK. Age-related differences in white matter tract microstructure are associated with cognitive performance from childhood to adulthood. *Biol Psychiatry*. 2014; 75:248–256. [PubMed: 23830668]
- Phillips KA, Rogers J, Barrett EA, Glahn DC, Kochunov P. Genetic contributions to the midsagittal area of the corpus callosum. *Twin Res Hum Genet*. 2012; 15:315–323. [PubMed: 22856367]
- Pinheiro J, Bates D, DebRoy S, Sarkar D, the R Core Team. nlme: Linear and Nonlinear Mixed Effects Models. R package version 3.1–88. 2008
- R-Development-Core-Team. R: A Language and Environment for Statistical Computing. Vienna, Austria: R Foundation for Statistical Computing; 2009.
- Repovs G, Csernansky JG, Barch DM. Brain network connectivity in individuals with schizophrenia and their siblings. *Biol Psychiatry*. 2011; 69:967–973. [PubMed: 21193174]
- Salthouse TA. Aging and measures of processing speed. *Biol Psychol*. 2000; 54:35–54. [PubMed: 11035219]
- Salthouse TA. When does age-related cognitive decline begin? *Neurobiol Aging*. 2009; 30:507–514. [PubMed: 19231028]
- Salthouse TA, Czaja SJ. Structural constraints on process explanations in cognitive aging. *Psychol Aging*. 2000; 15:44–55. [PubMed: 10755288]
- Schiavone F, Charlton RA, Barrick TR, Morris RG, Markus HS. Imaging age-related cognitive decline: A comparison of diffusion tensor and magnetization transfer MRI. *J Magn Reson Imaging*. 2009; 29:23–30. [PubMed: 19097099]
- Smith SM, Jenkinson M, Johansen-Berg H, Rueckert D, Nichols TE, Mackay CE, Watkins KE, Ciccarelli O, Cader MZ, Matthews PM, Behrens TE. Tract-based spatial statistics: Voxelwise analysis of multi-subject diffusion data. *Neuroimage*. 2006; 31:1487–1505. [PubMed: 16624579]
- Smith SM, Jenkinson M, Woolrich MW, Beckmann CF, Behrens TE, Johansen-Berg H, Bannister PR, De Luca M, Drobnjak I, Flitney DE, Niazy RK, Saunders J, Vickers J, Zhang Y, De Stefano N, Brady JM, Matthews PM. Advances in functional and structural MR image analysis and implementation as FSL. *Neuroimage*. 2004; 23(Suppl 1):S208–S219. [PubMed: 15501092]
- Susuki K. Node of Ranvier disruption as a cause of neurological diseases. *ASN Neuro*. 2013; 5:209–219. [PubMed: 23834220]
- Tingley D, Yamamoto T, Hirose K, Keele L, Imai K. Mediation: R Package for Causal Mediation Analysis. R package version. 2013; 4(3)
- Vaishnavi SN, Vlassenko AG, Rundle MM, Snyder AZ, Mintun MA, Raichle ME. Regional aerobic glycolysis in the human brain. *Proc Natl Acad Sci USA*. 2010; 107:17757–17762. [PubMed: 20837536]
- van Gelderen P, de Zwart JA, Duyn JH. Pitfalls of MRI measurement of white matter perfusion based on arterial spin labeling. *Magn Reson Med*. 2008; 59:788–795. [PubMed: 18383289]
- van Osch MJ, Teeuwisse WM, van Walderveen MA, Hendrikse J, Kies DA, van Buchem MA. Can arterial spin labeling detect white matter perfusion signal? *Magn Reson Med*. 2009; 62:165–173. [PubMed: 19365865]
- Wakana S, Jiang H, Nagae-Poetscher LM, van Zijl PC, Mori S. Fiber tract-based atlas of human white matter anatomy. *Radiology*. 2004; 230:77–87. [PubMed: 14645885]
- Wang J, Licht DJ. Pediatric perfusion MR imaging using arterial spin labeling. *Neuroimaging Clin N Am*. 2006; 16:149–167. ix. [PubMed: 16543090]

- Wang J, Alsop DC, Li L, Listerud J, Gonzalez-At JB, Schnall MD, Detre JA. Comparison of quantitative perfusion imaging using arterial spin labeling at 1.5 and 4.0 Tesla. *Magn Reson Med*. 2002; 48:242–254. [PubMed: 12210932]
- Wang J, Zhang Y, Wolf RL, Roc AC, Alsop DC, Detre JA. Amplitude-modulated continuous arterial spin-labeling 3.0-T perfusion MR imaging with a single coil: Feasibility study. *Radiology*. 2005; 235:218–228. [PubMed: 15716390]
- Waxman SG, Bennett MV. Relative conduction velocities of small myelinated and non-myelinated fibres in the central nervous system. *Nat New Biol*. 1972; 238:217–219. [PubMed: 4506206]
- Wechsler, D. Wechsler Adult Intelligence Scale. San Antonio, TX: Psychological Corporation; 1997.
- Weinberger DR. On the plausibility of “the neurodevelopmental hypothesis” of schizophrenia. *Neuropsychopharmacology*. 1996; 14:1S–11S. [PubMed: 8866738]
- Wen Q, Chklovskii DB. Segregation of the brain into gray and white matter: A design minimizing conduction delays. *PLoS Comput Biol*. 2005; 1:e78. [PubMed: 16389299]
- White T, Magnotta VA, Bockholt HJ, Williams S, Wallace S, Ehrlich S, Mueller BA, Ho BC, Jung RE, Clark VP, Lauriello J, Bustillo JR, Schulz SC, Gollub RL, Andreasen NC, Calhoun VD, Lim KO. Global white matter abnormalities in schizophrenia: A multisite diffusion tensor imaging study. *Schizophr Bull*. 2013; 37:222–232. [PubMed: 19770491]
- Wright SN, Kochunov P, Chiappelli J, McMahon RP, Muellerklein F, Wijtenburg SA, White MG, Rowland LM, Hong LE. Accelerated white matter aging in schizophrenia: Role of white matter blood perfusion. *Neurobiol Aging*. 2014; 35:2411–2418. [PubMed: 24680326]
- Yao L, Lui S, Liao Y, Du MY, Hu N, Thomas JA, Gong QY. White matter deficits in first episode schizophrenia: An activation likelihood estimation meta-analysis. *Prog Neuropsychopharmacol Biol Psychiatry*. 2013; 45:100–106. [PubMed: 23648972]

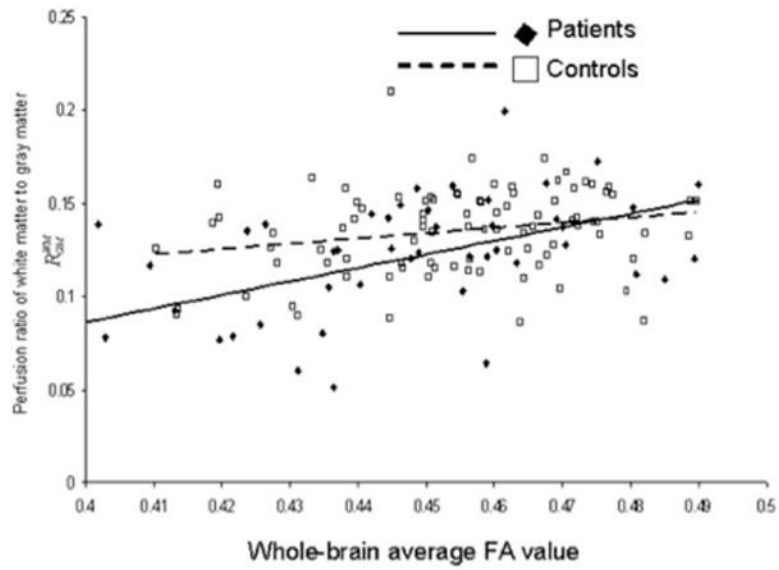


**Figure 1.** The perfusion ratio,  $R_{WM/GM}$ , was significantly correlated with the whole-brain average WM FA values in both groups ( $r = 0.52$ ,  $P = 0.0004$  and  $r = 0.25$ ,  $P = 0.05$ , for patients and controls, respectively).

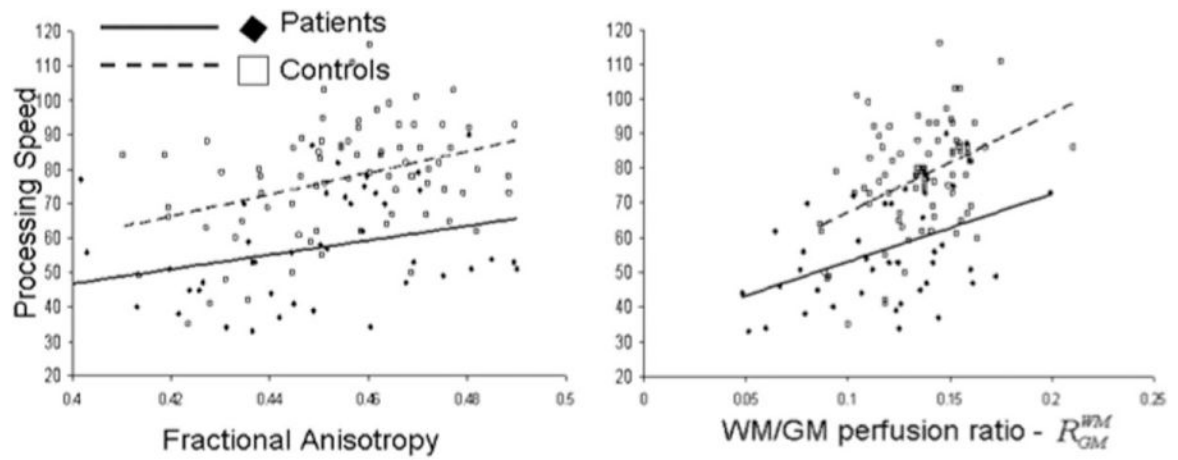


**Figure 2.**

Processing speed scores were plotted versus the whole-brain average FA (left) and  $R_{WM/GM}$  perfusion ratio (right) for cerebral WM. Processing speed scores were significantly correlated with FA values ( $r = 0.35$ ,  $P = 0.02$  and  $r = 0.36$ ,  $P = 0.005$ , in patients/controls, respectively) and with the  $R_{WM/GM}$  ratios ( $r = 0.44$ ,  $P = 4.5 \times 10^{-3}$  and  $r = 0.41$ ,  $P = 1.1 \times 10^{-3}$ , in patients/controls, respectively).

Clinical and demographic information for subjects used in this study

TABLE 1

Subjects	Average age, range (years)	Symptoms: BPRS	Processing speed	Age-of-onset (years)	Duration (years)	Weight (lb)	BMI	Current smokers	CBF whole brain <sup>a</sup>	CBF GM <sup>a</sup>	CBF WM <sup>a</sup>	GM: WM ratio	FA values	Working memory	WASI-IQ <sup>b</sup>
Patients (16F/30M)	37.5 ± 13.4, 19–59	2.1 ± .5	57.1 ± 16.8	18.6 ± 7.6	19.5 ± 13.5	188.8 ± 37.2	30.5 ± 6.2	30%	34.9 ± 8.4	56.9 ± 13.3	6.8 ± 2.4	9.2 ± 3.5	0.44 ± 0.02	17.5 ± 5.2	113.7 ± 12.6
Controls (26F/35M)	38.8 ± 14.3, 18–62	N/A	75.8 ± 15.8	N/A	N/A	184.2 ± 41.0	28.0 ± 4.8	23%	33.7 ± 6.8	54.0 ± 9.9	7.3 ± 2.0	7.6 ± 1.4	0.466 ± 0.02	20.7 ± 4.7	99.7 ± 17.7
Group difference, <i>P</i> -value	0.75		7.8 × 10 <sup>-8</sup>			0.34	0.25	0.32	0.34	0.5	0.17	2.5 × 10 <sup>-4</sup>	0.01	4.5 × 10 <sup>-4</sup>	0.003

There were no significant group differences in age and sex distribution for subjects with IQ scores.

<sup>a</sup>Perfusion measurements are in mL/100 mg/min.

<sup>b</sup>WASI-IQ scores were available for 77 subjects, including 24 patients (14 M, 10 F, 33.5 ± 13.7 years old) and 53 controls (24 M, 29 F, 34.9 ± 14.8 years old).

**TABLE II**

Results of the general linear model [Eq. (1)] analysis for processing speed and working memory

	Processing speed	Working memory
$\beta_{RWMGM}$ ( <i>P</i> -value)	219.05 ± 81.80 (0.01)	10.99 ± 25.91 (0.67)
$\beta_{FA}$ ( <i>P</i> -value)	0.03 ± 0.01 (0.004)	0.005 ± 0.004 (0.14)
<i>dx</i> ( <i>P</i> -value)	79.11 ± 67.68 (0.25)	76.68 ± 69.53 (0.27)
$\beta_{RWMGM \times dx}$ ( <i>P</i> -value)	-81.24 ± 107.07 (0.45)	32.35 ± 33.80 (0.34)
$\beta_{FA \times dx}$ ( <i>P</i> -value)	-0.02 ± 0.02 (0.24)	-0.004 ± 0.005 (0.46)
$r^2$	38%	14%
$F_{5,102}$ ( <i>P</i> -value)	13.13 ( $P = 10^{-9}$ )	4.43 ( $P = 0.01$ )

This model yielded the degree of variance explained, and tested the significance of the contribution from predictors to the variance in the PS. It also produced standardized coefficients ( $\beta$ ) that estimated linear associations between neurocognitive variables and predictors.

TABLE III

Results of the general linear model [Eq. (3)] analysis, where processing speed served as the dependent variable and regional WM to average GM CBF ratios and FA values for the ten WM tracts served as predictor variables

Processing Speed	Genu	Body	Splenium	IC	CR	TR	EC	Cing	SLF	FO
Patients										
$\beta$ Ratio CBF <sub>wm</sub> to CBF <sub>gm</sub> ( <i>P</i> -value)	212.83 ± 67.55 (3.1 × 10 <sup>-3</sup> )	158.94 ± 54.93 (6.2 × 10 <sup>-3</sup> )	159.57 ± 59.17 (0.01)	31.08 ± 58.25 (0.60)	216.09 ± 67.10 (2.6 × 10 <sup>-3</sup> )	68.86 ± 63.13 (0.28)	41.93 ± 57.27 (0.47)	91.20 ± 33.08 (8.8 × 10 <sup>-3</sup> )	91.43 ± 49.15 (0.07)	79.10 ± 45.35 (0.09)
$B_{FA}$ ( <i>P</i> -value)	-20.80 ± 46.65 (0.66)	1.20 ± 40.65 (0.98)	-65.33 ± 52.41 (0.22)	101.02 ± 118.31 (0.40)	50.59 ± 83.15 (0.55)	87.39 ± 68.92 (0.21)	97.09 ± 117.51 (0.41)	-15.23 ± 58.31 (0.80)	79.47 ± 88.23 (0.37)	99.55 ± 73.64 (0.18)
$r^2$	18%	22%	11%	0.01%	26%	7%	0.5%	14%	11%	8%
<i>F</i> ( <i>P</i> -value)	5.53 (7.7 × 10 <sup>-3</sup> )	6.73 (3.1 × 10 <sup>-3</sup> )	3.65 (0.04)	1.00 (0.38)	8.03 (1.2 × 10 <sup>-3</sup> )	2.62 (0.09)	1.12 (0.34)	4.21 (0.02)	3.63 (0.04)	2.7 (0.08)
Controls										
$\beta$ Ratio CBF <sub>wm</sub> to CBF <sub>gm</sub> ( <i>P</i> -value)	150.27 ± 43.11 (8.2 × 10 <sup>-4</sup> )	102.11 ± 33.39 (3.1 × 10 <sup>-3</sup> )	124.80 ± 44.24 (0.01)	135.99 ± 46.41 (4.5 × 10 <sup>-3</sup> )	124.29 ± 42.98 (0.01)	88.95 ± 44.78 (0.05)	105.69 ± 44.23 (0.02)	75.32 ± 20.58 (4.7 × 10 <sup>-4</sup> )	138.45 ± 42.32 (1.6 × 10 <sup>-3</sup> )	108.47 ± 31.56 (9.7 × 10 <sup>-4</sup> )
$\beta_{FA}$ ( <i>P</i> -value)	137.10 ± 36.35 (3.2 × 10 <sup>-4</sup> )	108.46 ± 38.65 (0.01)	238.40 ± 70.38 (1.1 × 10 <sup>-3</sup> )	131.35 ± 72.71 (0.07)	256.52 ± 67.85 (3.1 × 10 <sup>-4</sup> )	190.60 ± 54.57 (8.1 × 10 <sup>-4</sup> )	232.44 ± 78.61 (4.2 × 10 <sup>-3</sup> )	107.96 ± 50.90 (0.04)	167.68 ± 68.97 (0.02)	116.12 ± 57.64 (0.05)
$r^2$	26%	18%	19%	11%	19%	18%	13%	18%	16%	15%
<i>F</i> ( <i>P</i> -value)	14.47 (4.9 × 10 <sup>-6</sup> )	9.58 (2.0 × 10 <sup>-4</sup> )	10.19 (1.2 × 10 <sup>-4</sup> )	5.65 (0.01)	9.93 (1.5 × 10 <sup>-4</sup> )	9.52 (2.1 × 10 <sup>-4</sup> )	6.76 (2.0 × 10 <sup>-3</sup> )	9.24 (2.6 × 10 <sup>-4</sup> )	8.14 (6.4 × 10 <sup>-4</sup> )	7.69 (9.2 × 10 <sup>-4</sup> )

This modeling was performed for patient and control groups.

The WM tracts were abbreviated as follows: IC, internal capsule; CR, corona radiata; TR, thalamic radiata; EC, external capsule; Cing, cingulate; SLF, superior longitudinal fasciculus; FO, superior and inferior fronto-occipital fasciculi.